Ambipolar organic light-emitting transistors employing heterojunctions of n-type and p-type materials as the active layer

2006 J. Phys.: Condens. Matter 18 S2127

(http://iopscience.iop.org/0953-8984/18/33/S28)

INSTITUTE OF PHYSICS PUBLISHING JOURNAL OF PHYSICS: CONDENSED MATTER

J. Phys.: Condens. Matter **18** (2006) S2127–S2138 doi:10.1088/0953-8984/18/33/S28

Ambipolar organic light-emitting transistors employing heterojunctions of n-type and p-type materials as the active layer

R Capelli[1], **F Dinelli, M A Loi, M Murgia, R Zamboni and M Muccini**

Consiglio Nazionale delle Ricerche (CNR), Istituto per lo Studio dei Materiali Nanostrutturati (ISMN), via P Gobetti 101, I-40129 Bologna, Italy

E-mail: R.Capelli@bo.ismn.cnr.it

Received 31 January 2006, in final form 30 March 2006
Published 4 August 2006
Online at stacks.iop.org/JPhysCM/18/S2127

Abstract

The realization of organic light-emitting transistors (OLETs) with high quantum efficiency and fast switching time is crucial for the development of highly integrated organic optoelectronic systems. In order to reach such a goal, fabrication of devices with ambipolar transport and high charge mobility values is needed. At present, organic materials having intrinsically ambipolar transport are restricted in number and show poor performance. This limits their use in efficient and fast switching single layer ambipolar OLETs. In this framework, we have taken the approach of combining p-type and n-type materials in two complementary configurations. The first one is based on realizing layered structures (bi-layer heterojunction) where materials are sequentially deposited. The second one is based on simultaneously evaporating two materials with variable composition (bulk heterojunction) to form a mixed film. In this paper, the charge transport and electroluminescence properties of OLETs based on these heterostructures are presented. A correlation between the active layer structure and the electrical performances has been obtained by means of laser scanning confocal microscopy, here employed for morphology and spectroscopy analysis. Differences between the two approaches are critically discussed.

(Some figures in this article are in colour only in the electronic version)

1. Introduction

Organic field-effect transistors (OFETs) and organic light-emitting diodes (OLEDs) are nowadays well established devices with performances comparable to the equivalent inorganic

[1] Author to whom any correspondence should be addressed.

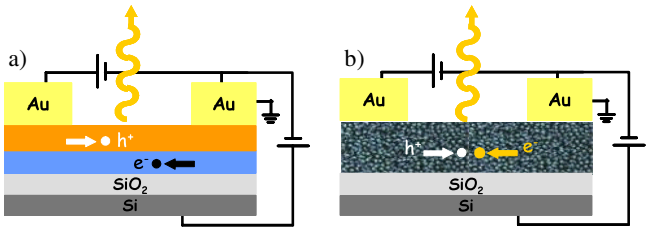

Figure 1. Schematics of OLET devices based on the bi-layer heterojunction (a) and on the bulk heterojunction (b).

ones [1]. Commercial applications are starting to appear on the market [2]. Recently the possibility of obtaining light emission together with good transport properties in OFETs has been also demonstrated [3, 4]. This opens the perspective of fabricating fully integrated devices (organic light-emitting transistors, OLETs) combining electrical switching and light emission, with low fabrication costs and high integration potential in organic and hybrid chips.

The first OLETs reported in the literature were operated in the unipolar charge conduction regime, i.e., with only one type of charge carrier (electrons or holes) flowing through the channel. Radiative recombination is thus confined to a spatial region near the drain metal electrode where the complementary charge carriers are injected [4]. This represents one of the main drawbacks of this approach. An alternative strategy to enhance device performances is represented by employing ambipolar OLETs. In this case both electrons and holes flow through the organic film and the excitons are formed by the recombination of the charge carriers within the transport layer. The main advantage of this approach consists in the fact that the distribution and the density of the charge carriers may be controlled via the intrinsic electron and hole mobility and the device operating conditions, namely the gate bias. In this way the exciton formation process and light emission can be optimized. Examples of OLETs employing a polymer film showing intrinsic ambipolar transport have been reported in the literature [5, 6]. The location of the recombination region far from the device electrodes prevents the excitons from being quenched due to the interaction with the metallic contacts. However these OLETs are characterized by low mobility values for both charge carriers ($\approx 10^{-4}$ cm^2 V^{-1} s^{-1}), affecting the electrical switching performances and limiting their applications as electronic devices. Additionally, with concern to the light generation, high mobility values are needed to reduce exciton quenching due to the interaction with free charges flowing in the transport region.

At present, charge mobility values comparable with those of amorphous silicon devices (≈ 1 cm^2 V^{-1}s^{-1}) have been obtained only with small molecules. However, most of the molecular systems used in organic electronics show unipolar field-effect charge transport. Examples of intrinsic ambipolar transport are nowadays restricted to a few materials with limited performances and significant sensitivity to the environmental conditions [7–10]. An alternative to the quest for intrinsic ambipolar transport is given by the two-material approach, where a p-type material is combined with an n-type material. In this way, it is possible to combine the best performing single unipolar materials to obtain ambipolar OLETs with good electrical and switching performance. In the following, we present ambipolar OLETs based on the combination of two organic materials reaching, in the best cases, a balanced transport and charge mobility of the order of 10^{-2} cm^2 V^{-1}s^{-1}.

The first configuration considered is based on a bi-layered structure [11]. Hole and electron transport films are grown sequentially on the substrate. The interaction between p-type and

n-type molecules is limited to the interface between the two layers. In the second structure, p-type and n-type molecules are simultaneously sublimed [12]. The film obtained in this way results in a homogeneous mixture of the two materials. The interface between p-type and n-type molecules is now extended to a tri-dimensional region. Advantages and drawbacks of the two approaches are herein discussed.

2. Experimental details

Pentacene, α-quinquethiophene (T5) and N,N'-ditridecylperylene-3,4,9,10-tetracarboxylic diimide (PTCDI-$C_{13}H_{27}$, P13) were purchased from Aldrich and employed as received. DH4T was synthesized as described in [8]. Organic films were deposited at a base pressure of 5×10^{-7} mbar. Substrates consisted of heavily doped n^{2+} silicon with a layer of thermally grown oxide. The oxide thickness varied from 100 to 300 nm ($C_{ox} = 36$–12×10^{-9} F cm^{-1}, respectively). No surface treatment was carried out on the oxide apart from cleaning procedures such as sonication in chloroform or isopropanol, acetone and UHP water in order to remove adventitious organic contamination. OLET devices were fabricated in the top electrode configuration. The electrodes, 50–70 nm thick, were made of gold deposited at a base pressure of 2×10^{-4} mbar at a growth rate of 0.5 Å s^{-1} with the sample held at room temperature or -120 °C. Device geometry factors were the following: width (W) = 10 000 μm and length (L) = 150–600 μm for the layered heterojunctions, W = 55 000 μm and L = 40 μm for the bulk heterojunctions. Mobility and threshold voltage values were evaluated in the saturation regime via acquisition of locus curves. When not limited by the contact resistance at the organic/electrode interfaces, they were also calculated in the linear regime from the transfer curves. The results were essentially indistinguishable.

In layered heterojunctions, the deposition parameters of DH4T, pentacene and P13 were optimized for each material in a single layer configuration. The substrate temperature (T_{sub}) values for film growth were: 90 °C for DH4T; 25 °C for P13; 50 °C for pentacene. The growth rate was fixed for all materials at 0.1–0.2 Å s^{-1} (0.6–1.2 nm min^{-1}), each layer with a nominal thickness of 20 nm (as measured by quartz microbalance). The electrical measurements were carried out in an integrating sphere at a base pressure of 1×10^{-4} mbar using a photomultiplier for electroluminescence (EL) measurements.

The bulk heterojunctions were prepared by co-evaporation of T5 and P13 with variable volume ratios and a total thickness of about 50 nm. The deposition rate was kept constant at 0.1 Å s^{-1} for each material. The different volume ratios were obtained by reducing the flux of one of the components with a mechanical chopper. The relative concentrations of the two materials are nominal values; small variations between different depositions can occur. The electrical measurements were carried out in an Ar glove box (<1 ppm O_2, H_2O); the transistor output and transfer characteristics as well as the photocurrent were measured with an Agilent 4155C semiconductor parameter analyser.

Laser scanning confocal microscopy (LSCM) was performed with a set-up based on a Nikon Eclipse 2000-E laser scanning confocal microscope working in the backscattering configuration [13]. Photoluminescence was excited with the 488 nm Ar^+ laser line. Sample imaging was achieved by rastering the laser spot on the sample surface and by detecting, point-by-point, the sample photoluminescence with two photomultipliers centred in the green (515 $\pm$ 20 nm) and red spectral range (>600 nm), respectively. PL emission for time-resolved and steady-state measurements was excited by the second harmonic (400 nm) of a Ti:sapphire laser delivering 100 fs pulses. The signal was recorded by a Hamamatsu streak camera with $\sim$2 ps time resolution.

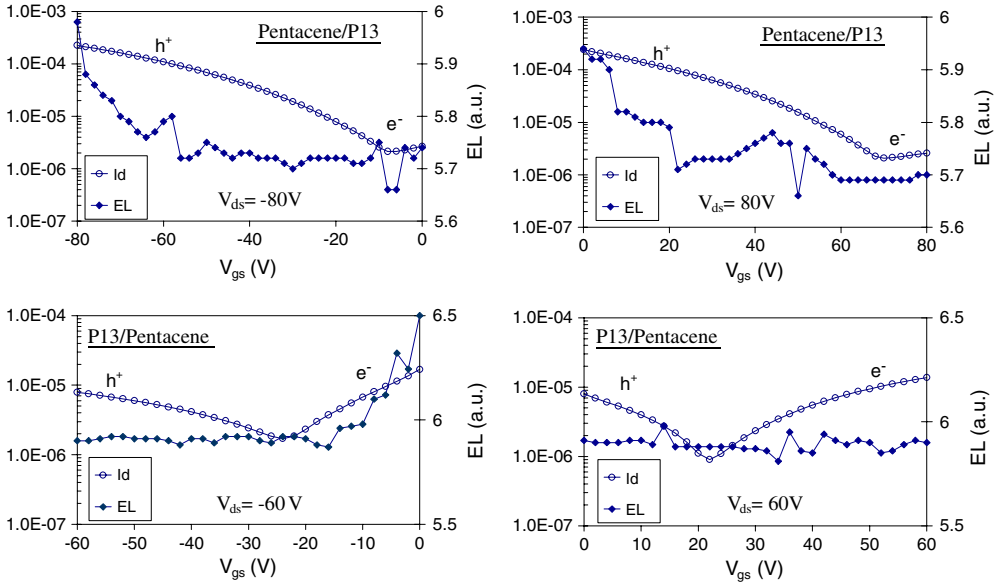

Figure 2. Transfer characteristics of OLET devices based on Pentacene/P13 and P13/Pentacene bi-layers with the corresponding EL data. The V_{ds} values are reported besides each curve. The symbols 'e^-' and 'h^+' are used to indicate the prevailing type of charge carriers forming I_d for different biasing conditions.

3. Results and discussion

3.1. Bi-layer heterojunction OLETs

In this configuration, a p-type material film is superimposed to a n-type one placed in direct contact with the dielectric surface (see figure 1) or vice versa. This approach presents the advantage of enhanced charge transport and mobility values. It is known that in OFETs the charge transport is confined to the first few layers next to the dielectric [14]. Thus, electron and hole paths are confined at the interface between the first layer and the substrate and at the interface between the two organic films. If the two films are continuous, the charge transport should be uniform in both films over all the device channel area and therefore good transport properties are expected.

Data herein reported refer to devices where the p-type film was made of dihexyl-quaterthiophene (DH4T) or pentacene molecules. For the n-type transport layer we employed N,N'-ditridecylperylene-3,4,9,10-tetracarboxylic diimide, PTCDI-$C_{13}H_{27}$ (P13) molecules. Pentacene is the p-type material showing the best mobility in single layer OFETs ($\sim$1 cm^2 V^{-1}s^{-1}) [1] while DH4T is a good p-type material with mobility above 10^{-2} cm^2 V^{-1}s^{-1} [8]. On the other hand, P13 is one of the best n-type material in terms of electron mobility in single layer OFETs ($\sim$0.1 cm^2 V^{-1}s^{-1}) [11, 15]. In order to explore the influence of the bottom layer on the morphology of the upper layer, and therefore on the quality of the interface between the two layers, we changed the sequence of sublimation and also the p-type material. The four configurations considered in the following are obtained by sequentially depositing pentacene and P13 films (Pentacene/P13), P13 and pentacene films (P13/Pentacene), DH4T and P13 films (DH4T/P13), P13 and DH4T films (P13/DH4T).

In figure 2 we report the transfer characteristics (drain current, I_d, versus gate–source voltage, V_{gs}) of Pentacene/P13 and P13/Pentacene devices together with the

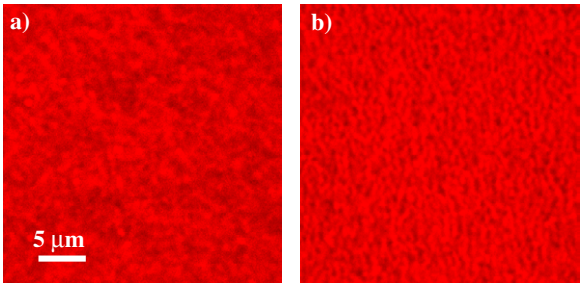

Figure 3. LSCM images of P13 films: (a) in Pentacene/P13 and (b) in P13/Pentacene heterojunctions.

electroluminescence (EL) data. The drain–source voltage (V_{ds}) is set to operate in the saturation regime. In the graphs we have also indicated the type of carriers (electrons, e^-, and holes, h^+) injected either from the drain or source electrode, depending on the biasing values. The asymmetry in the current signal (figure 2, top) [11] shows that Pentacene/P13 devices exhibit an unbalanced transport with a hole mobility (μ^p) comparable to that of single layer OFETs (0.2–0.4 $cm^2\ V^{-1}s^{-1}$) but with an electron mobility (μ^n) lower by two orders of magnitude (0.002 $cm^2\ V^{-1}s^{-1}$) with respect to single layer devices. P13/Pentacene devices show a balanced transport (figure 2, bottom) but μ^n is one order of magnitude lower than the single layer OFET values (0.015 $cm^2\ V^{-1}s^{-1}$) and μ^p almost two orders of magnitude lower than single layer OFET values (0.012 $cm^2\ V^{-1}s^{-1}$). These differences related to the inversion of the deposition sequence are likely due to differences in growth modality on a surface different from silicon oxide both in morphology and chemical composition.

EL has been revealed only for the P13/Pentacene configuration in coincidence with electron transport. The EL signal increases with increasing electron current. The same behaviour was observed in unipolar OLETs [3, 4]. This allows us to conclude that, also in this case, EL is confined to a region near the drain electrode. This means that the spatial separation between the electron and the hole transport layers, in spite of the electron–hole attraction, reduces drastically the probability of exciton formation inside the device channel.

In order to explain these variations, a morphological analysis of the layered structures was performed. We have employed laser scanning confocal microscopy (LSCM), in which samples are scanned with a laser and the resulting photoluminescence (PL) collected. The advantage of using this technique is that the laser excitation penetrates inside the device channel allowing the observation not only of the outermost but also of buried layers. From the PL images one can then deduce the morphological characteristics of the various interfaces. Concerning single layer OTFTs, pentacene is known to grow in a layered manner forming terrace-like structures on silicon oxide surfaces [16]. On the other hand, P13 molecules form continuous films [12].

LSCM images of Pentacene/P13 and P13/Pentacene combinations are displayed in figure 3. The pentacene PL signal is too low to be collected so, in figure 3, we report only images of the P13 film when grown at the bottom or at the top of the bi-layer structure. It is evident that, while forming a continuous film on the bare silicon substrate, P13 films are discontinuous when deposited on pentacene. The morphology appears to be web-like with empty holes. We conclude that the lack of film continuity is at the origin of the worsening of electron transport in Pentacene/P13 devices. Although we cannot image pentacene layers grown on P13 films, we infer from the dropping of μ^p in P13/Pentacene devices that pentacene films are less ordered and/or continuous when grown on P13. These data indicate that the

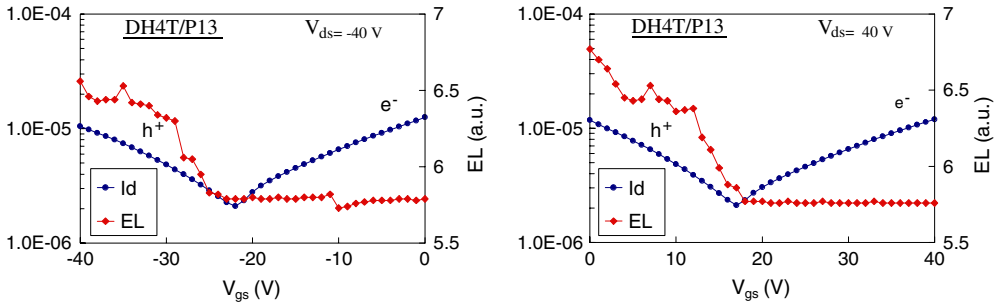

Figure 4. Transfer characteristics of an OLET device based on a DH4T/P13 heterojunction with the correspondent EL data. The V_{ds} values are reported besides each curve. The symbols 'e^-' and 'h^+' are used to indicate the prevailing type of charge carriers forming I_d for different biasing conditions.

material choice in order to form smooth and continuous organic/organic interfaces is not trivial and that optimum properties are not necessarily obtained by employing the best performing materials in single layer configurations.

The importance of growth compatibility between the organic layers in OLETs based on a bi-layer structure is further confirmed by the results concerning the DH4T/P13 and P13/DH4T configurations. In figure 4 we report the transfer characteristics of DH4T/P13 devices and the correspondent EL. We can see that the electron and the hole currents are well balanced ($\mu \sim 3 \times 10^{-2}$ cm^2 V^{-1}s^{-1} for both types of conduction). μ^p does not vary substantially with respect to single layer devices, while μ^n falls by one order of magnitude despite the fact that P13 growth is carried out under optimized conditions [11]. EL occurs in correspondence to hole transport and increases with increasing current as in the case of Pentacene/P13 devices.

The output characteristics of the P13/DH4T configuration, not reported here, exhibit an unbalanced transport: electron transport is more pronounced than hole transport as μ^p drops by one order of magnitude with respect to the DH4T/P13 device. EL occurs in correspondence to electron transport and is proportional to the current. We can conclude that in OLETs based on a bi-layer structure EL is always related to charge transport in the layer directly in contact with the substrate. When charges are accumulated along the channel device at the interface between the silicon substrate and the organic film, the superposition of bi-layer/drain contact near the drain top electrode is likely to form an OLED structure. In all the other cases, the spatial separation between holes and electrons prevents an efficient electron–hole recombination and light emission.

The good results in terms of charge balancing and carrier mobility obtained in the DH4T/P13 configuration are related to the fact that the DH4T film surface allows favourable conditions for the P13 growth. This is evidenced from the LSCM analysis of the bi-layer morphology. In single layer OFETs, DH4T is characterized by a layer-by-layer growth [17]. In figures 5(a) and (b), the LSCM images reveal that the morphology of the DH4T film grown on P13 is discontinuous compared to the DH4T film grown directly on the dielectric. In figures 5(c) and (d), in contrast, the PL images evidence that the P13 films are continuous, independently of whether they are deposited on the dielectric or on DH4T. Within the resolution limits of LSCM, the morphology is also very similar. Thus, P13 can form continuous films on either silicon oxide or DH4T, but DH4T cannot form a continuous film on P13. This plausibly explains the device characteristics reported above. Associated with an interfacial discontinuity in the organic films there is a deterioration in charge transport efficiency.

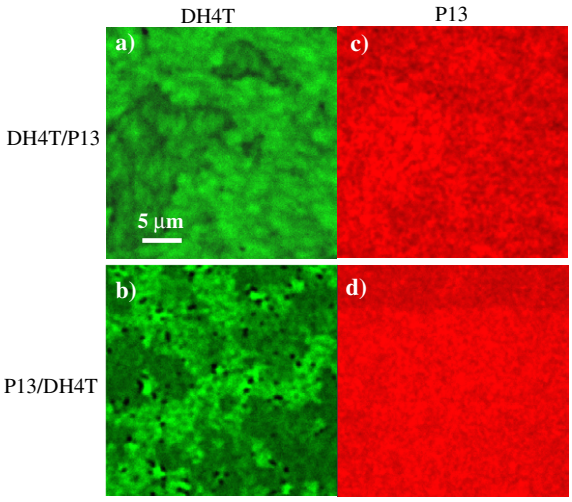

Figure 5. LSCM images of DH4T/P13 ((a), (c)) and P13/DH4T ((b), (d)) heterojunctions. PL collected from DH4T is reported in (a) and (b), and PL from P13 in (c) and (d).

3.2. Bulk heterojunction OLETs

In bulk heterojunction OLETs, p-type molecules and n-type molecules are mixed together via co-evaporation of the two materials on the same substrate (see figure 1) [12]. Compared to the bi-layer configuration, this approach presents one main advantage: the electron and hole flows are interpenetrated in the charge transport region and the interface between the p-type and n-type materials is much more extended. This augments the probability that electrons and holes recombine to form excitons. However, a reduction of the charge mobility is to be expected, as the charge transport layer located next to the dielectric surface lacks continuity and possibly molecular order compared to single layer OFETs.

The bulk heterojunctions herein presented are composed of N,N'-ditridecylperylene 3,4,9,10-tetracarboxylic diimide (P13) for electron conduction and α-quinquethiophene (T5) for hole conduction. T5 is known as a good hole-transporting material [18]. The two materials were chosen because the relative positions of their highest occupied (HOMO) and the lowest unoccupied molecular orbitals (LUMO) allow exciton formation and recombination in the material with smaller energy gap (P13 in this case). To investigate the influence of the relative composition on mobility and EL, OFETs with varying T5:P13 volume ratio have been investigated. Output and transfer characteristics of a device with a T5:P13 ratio of 1:3 are shown in figure 6 together with the corresponding EL intensity. Although the output characteristic shows no indication of ambipolar transport, EL occurs for both V_{ds} polarities. μ^n is about one order of magnitude lower than in single layer OFETs [12b].

Figure 7 shows the transfer characteristics with the corresponding EL intensity of a bulk heterojunction OLET with a volume ratio 1:1. In this case the device exhibits a pronounced ambipolar behavior in the output and transfer characteristics, as discussed in detail in [12]. μ^p is more than one order of magnitude lower with respect to single layer OFETs (5×10^{-4} cm^2 V^{-1}s^{-1}) and μ^n drops by about one order of magnitude (1×10^{-3} cm^2 V^{-1}s^{-1}). The EL behaviour, as a function of V_{ds} in the transfer curves of figures 6 and 7, is what we could expect when excitons are formed inside the channel device, far from the drain contact, by the direct interaction between p-type and n-type molecules dispersed in the bulk heterojunction.

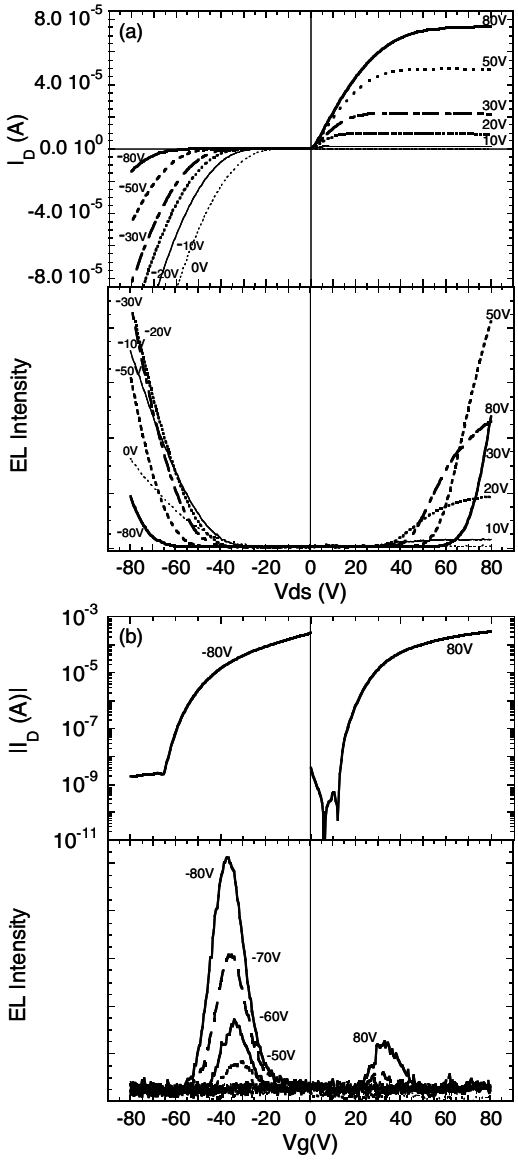

Figure 6. Output and transfer characteristics of an OLET device based on a bulk heterojunction with a T5/P13 ratio of 1:3 with the correspondent EL data. The V_{gs} (a) and V_{ds} (b) values are reported next to each curve.

The devices with an excess of T5, e.g. T5:P13 ratios of 3:1 and 9:1, show ambipolar transport but no EL.

μ^n and μ^p are plotted as a function of composition ratio in figure 8. They both decrease exponentially if the relative concentrations of the electron- and the hole-transporting material are decreased from 100 to 50%. μ^n decreases in this range by one order of magnitude, whereas μ^p decreases by 1.5 orders of magnitude. At lower concentrations, μ^n seems to level off, whereas μ^p is below the detection limit. Electron as well as hole flows, i.e. ambipolar transport,

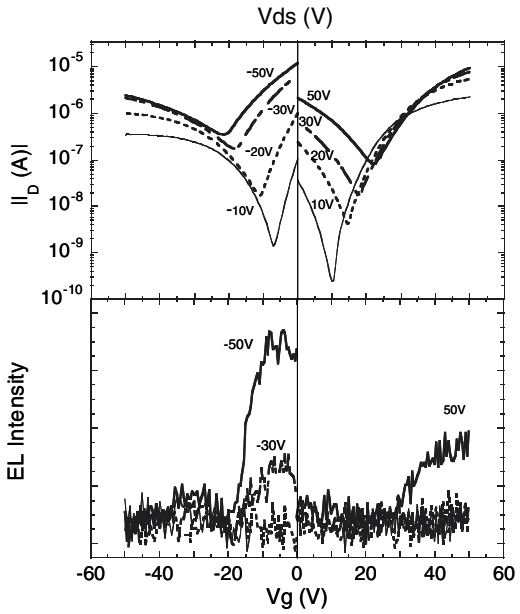

Figure 7. Transfer characteristics of an OLET device based on a bulk heterojunction with a T5/P13 ratio of 1:1 with the correspondent EL data. The V_{ds} values are reported next to each curve.

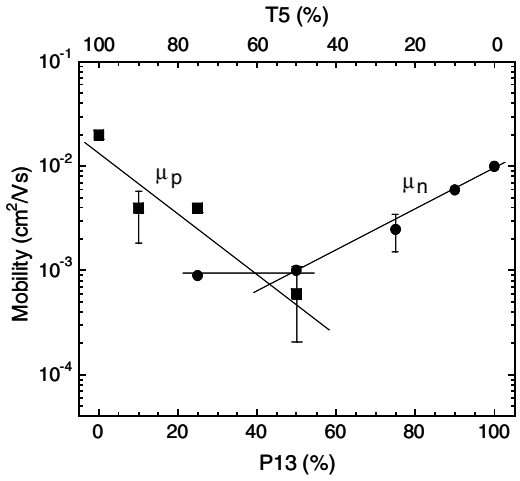

Figure 8. Hole and electron mobility of bulk heterojunction OLETs are plotted versus T5 and P13 percentage.

on the same sample could only be measured for T5:P13 ratios of 1:1 and 3:1. A perfect balance of μ^n and μ^p is extrapolated for a T5:P13 ratio of roughly 3:2, as shown in figure 8.

To obtain a better understanding of the bulk heterojunction OFET properties, the morphology of the films and the recombination process of the excited states were studied by means of LSCM and time-resolved PL spectroscopy. Transient PL decay of films with different P13 content is shown in figure 9. The PL dynamics of P13 in the bulk heterojunction

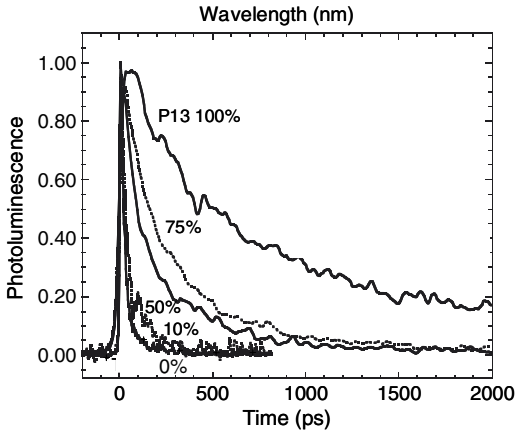

Figure 9. PL transients of pure P13 and T5 films and of bulk heterojunctions with different T5/P13 ratios.

films strongly depends on the T5:P13 ratio. The decay of pure P13 films is bi-exponential, with a first decay time $\tau_1 \approx 350$ ps and a tail $\tau_2 \approx 1.6$ ns [12b]. The dynamics of the P13 emission in the co-evaporated films with increasing percentages of T5 becomes extremely fast, up to $\tau_1 \approx 20$ ps and $\tau_2 \approx 100$ ps. These decay times are typical of neat T5 films, which are characterized by H-type aggregation where efficient non-radiative recombination is responsible for the low PL efficiency.

The observed PL dynamics and quenching of the P13 emission can be considered a sign of exciton dissociation by hole transfer to the material having the lower ionization potential (T5). An alternative explanation for the observed P13 lifetime variation due to energy transfer from P13 to T5 is to be ruled out because the higher energy gap of T5 with respect to that of P13 prevents the process from occurring. The quenching process competes with exciton recombination and hence light emission in bulk heterojunctions. This phenomenon, predominant at high T5 concentrations, explains why OFETs with an excess of T5 present no EL emission although the transistor characteristics exhibit clear ambipolar transport.

Further insights into the device working mechanisms can be obtained from morphology investigations. In figures 10(a) and (a′), the LSCM micrographs for the red and the green spectral range of the co-evaporated film with a T5:P13 volume ratio of 3:1 are presented. The morphology of the film is rather inhomogeneous, and the bulk heterojunction is dominated by large T5 clusters $\sim$1 μm in size. From the LSCM micrographs, it can be concluded that T5 and P13 do not mix on a molecular scale in the co-evaporated thin films, but form an interconnected network of micro- and nano-crystalline clusters. In particular the tendency of T5 to form clusters is in good agreement with the observation of bulk T5 PL spectra in the co-evaporated films rather than the solution spectra [19].

Comparing the LSCM information with the electrical characteristics of the bulk heterojunction OLETs with varying compositions of T5 and P13 allows some conclusions on the microscopic structure of the heterojunction and the resulting current percolation. A relative content of 25% of P13 is sufficient to obtain a continuous path for electrons resulting in a measurable electron mobility. An equivalent content of T5 is not enough to achieve comparable hole conduction. This can be explained by the different growth mechanisms of the two materials. As T5 tends to form clusters, it is very likely that the percolation threshold to create a continuous pathway for holes is larger than 25%. In contrast, for the highly surface-mobile P13

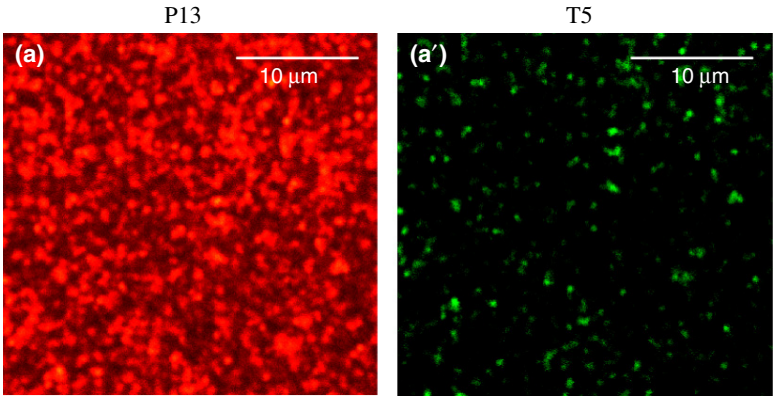

Figure 10. LSCM images of a bulk heterojunction with T5/P13 ratios of 3:1. The PL of P13 is detected in the red spectral range, while the PL of T5 is detected in the green spectral range.

molecules, we conclude that the percolation threshold is lower than 25%. Thus, even diluted concentrations of P13 lead to continuous pathways for electrons in the bulk heterojunction. As a result of the cluster formation, it can be concluded that whether charge separation or light emission is the predominant phenomenon in T5/P13 bulk heterojunction depends critically on the ratio and dispersion of the two components.

4. Conclusions

In this paper we have demonstrated that OLETs with balanced ambipolar transport can be fabricated by combining together p-type and n-type materials. Two types of structure have been proposed: layered and bulk heterojunctions. The bi-layer heterojunction approach allows one to obtain electron and hole mobility values above 10^{-2} cm^2 V^{-1}s^{-1}, provided that there is growth compatibility between the two materials. However, electroluminescence results confined next to the drain metal electrode like in the case of unipolar OLETs. The bulk heterojunction approach moves the electron–hole recombination region inside the channel and far from the electrodes. However, the most balanced charge transport is obtained with lower mobility values of the order of 10^{-3} cm^2 V^{-1}s^{-1}.

We believe that the improvements achieved in terms of mobility and charge balance in ambipolar transport and the good control in charge mobility obtained with organic heterojunctions provide useful information for the future developments of OLET technology. The next challenge is to combine the advantages of the two heterojunction approaches. It is also crucial to select material combinations allowing one to improve the electroluminescence efficiency.

Acknowledgments

The authors acknowledge useful discussions with Antonio Facchetti, Tobin J Marks, Constance Rost-Bietsch and Siegfried Karg. This work was supported by EU under project FP6-IST-015034 (OLAS) and by Italian Ministry MIUR under project FIRB—RBNE033KMA ‘Composti molecolari e materiali ibridi nanostrutturati con proprietà ottiche risonanti e non risonanti per dispositivi fotonici’.

References

[1a] Nelson S F, Lin Y-Y, Gundlach D J and Jackson T N 1998 *Appl. Phys. Lett.* **72** 1854
[1b] Klauk H, Halik M, Zschieschang U, Schmid G and Radlik W 2002 *J. Appl.* **92** 5259
[2a] Hung L S and Chen C H 2002 *Mater. Sci. Eng.* **39** 143
[2b] Malliaras G and Friend R 2005 *Phys. Today* **58** 53
[3] Hepp A, Heil H, Weise W, Ahles M, Schmechel R and von Seggern H 2003 *Phys. Rev. Lett.* **91** 157406
[4] Santato C, Capelli R, Loi M A, Roy V A L, Stallinga P, Cicoira F, Murgia M, Zamboni R, Muccini M, Rost C and Karg S 2004 *Synth. Met.* **146** 329
[5] Zaumseil J, Friend R and Sirringhaus H 2006 *Nat. Mater.* **5** 69
[6] Swensen J S, Soci C and Heeger A J 2005 *Appl. Phys. Lett.* **87** 253511
[7] Yasuda T and Tsutsui T 2005 *Chem. Phys. Lett.* **402** 395
[8] Yoon M-H, Di Benedetto S A, Facchetti A and Marks T 2005 *J. Am. Chem. Soc.* **127** 1348
[9] Anthopulos T G, Tanase C, Setayesh S, Meijer E J, Hummelen J C, Blom P W and de Leeuw D 2004 *Adv. Mater.* **16** 2174
[10] Meijer E J, de Leeuw D M, Setayesh S, van Veneendaal E, Huisman B-H, Blom P W M, Hummelen J C, Scherf U and Klapwijk T M 2003 *Nat. Mater.* **2** 678
[11] Dinelli F, Capelli R, Loi M A, Murgia M, Muccini M, Facchetti A and Marks T J 2006 *Adv. Mater.* **18** 1416
[12a] Rost C, Karg S, Riess W, Loi M A, Murgia M and Muccini M 2004 *Appl. Phys. Lett.* **85** 1613
[12b] Loi M A, Rost-Bietsch C, Murgia M, Karg S F, Riess W and Muccini M 2006 *Adv. Funct. Mater.* **16** 41
[13a] Loi M A, da Como E, Zamboni R and Muccini M 2003 *Synth. Met.* **139** 687
[13b] Loi M A, Da Como E, Dinelli F, Murgia M, Zamboni R, Biscarini F and Muccini M 2005 *Nat. Mater.* **4** 81
[14] Dinelli F, Murgia M, Levy P, Cavallini M, Biscarini F and de Leeuw D 2004 *Phys. Rev. Lett.* **92** 6802
[15] Gundlach D J, Pernstich K P, Wilckens G, Gruter M, Haas S and Batlogg B 2005 *J. Appl. Phys.* **98** 4502
[16] Meyer zu Heringdorf J F, Reuter M C and Tromp R M 2003 *Nature* **412** 517
[17] Muck T, Wagner V, Bass U, Leufgen M, Geurts J and Molenkamp L W 2004 *Synth. Met.* **146** 317
[18] Melucci M, Gazzano M, Barbarella G, Cavallini M, Biscarini F, Maccagnani P and Ostoja P 2003 *J. Am. Chem. Soc.* **125** 10266
[19] Loi M A, Mura A, Bongiovanni G, Botta C, Di Silvestro G and Tubino R 2001 *Synth. Met.* **121** 1299